

Improvement of Brain Tumors Detection Using Markers and Boundaries Transform

Yousif Mohamed Y. Abdallah^{1,2}, Mommen A. Alkhir³, Amel S. Algaddal⁴

¹College of Applied Medical Science, Almajmah University, Riyadh, Saudi Arabia

²Sudan University of Science and Technology, College of Medical Radiological Science, Khartoum, Sudan

³College of Applied Medical Science, Sebha University, Libya

⁴Sebha Infertility Center, Sebha, Libya

Abstract: *This was experimental study conducted to study segmentation of brain in MRI images using edge detection and morphology filters. For brain MRI images each film scanned using digitizer scanner then treated by using image processing program (MatLab), where the segmentation was studied. The scanned image was saved in a TIFF file format to preserve the quality of the image. Brain tissue can be easily detected in MRI image if the object has sufficient contrast from the background. We use edge detection and basic morphology tools to detect a brain. The segmentation of MRI images steps using detection and morphology filters were image reading, detection Entire brain, Dilation of the image, filling interior gaps inside the image, removal connected objects on borders and smoothen the object (brain). The results of this study were that it showed an alternate method for displaying the segmented object would be to place an outline around the segmented brain. Those filters approaches can help in removal of unwanted background information and increase diagnostic information of Brain MRI.*

Keywords: Improvement, brain, Matlab, Markers and Boundaries

1. Introduction

Functional brain imaging can be strictly or more broadly defined. We consider it broadly to include the full range of techniques by which physiological changes accompanying brain activity are defined. Different techniques are sensitive to different types of changes. In contrast to many of the in vitro methods used to define brain function, methods used in vivo generally are concerned not with the behaviours of single neurones but with the activities of large populations of neurones. This nonetheless is highly informative, as single neurones do not work independently, but function in large aggregates (consider, for example, the vertical integration of neurones in columns in primary sensory cortex). Despite the small sizes of individual neurones, useful information concerning brain function therefore can be obtained using methods that have an in-plane spatial resolution of even 3 mm or greater. Information transfer in the brain along axons occurs by electrical conduction. Information is transferred between neurones by the release of neurotransmitter molecules at synapses and their subsequent interactions with specific receptors on target neurones. These neurotransmitter-receptor interactions then lead to changes in membrane current flow which change the post-synaptic neuronal membrane potential (and the accompanying extracellular electrical field) and alter depolarization frequency. The metabolic changes in neurones and glia that accompany neurotransmitter release are energy-requiring. Most of this energy is used at or around synapses. As normal brain energy production depends ultimately on oxidative metabolism, there thus is greater local demand for delivery of oxygen with increased synaptic activity. To meet this increased metabolic demand, neuronal activation is accompanied by increased local blood flow. In 1890 the

physiologist Charles Sherrington demonstrated that stimulation of the brain caused a local increase in blood flow. However, he also observed that the relative proportion of oxygen extracted from this blood was reduced: the increase in total oxygen delivery exceeded the increase in oxygen utilization. There are three basic means by which radiologic images are produced: transmission of energy, reflection of energy, and emission of energy. The so-called x-ray or radiograph is produced by the transmission of energy. A beam of high-energy photons is passed through the body, some of which are attenuated or blocked when they strike subatomic particles. The higher the atomic weight of the substance through which the photons are passing, the "denser" it appears to photons, and the more likely they are to be blocked, or attenuated. In decreasing order of density, the principal densities visible in a radiograph are metal, bone, water (including soft tissues such as muscle), fat, and air. Of course, even though muscle is denser than fat, the x-ray beam would be more attenuated by passing through a meter of fat than a centimeter of muscle. Both density and thickness, then, are factors to take into account in assessing the degree of opacification noted on a radiograph (Fig. 1–5). Radiographs were initially referred to as "skiagraphs," from the Greek for "shadow pictures," because they represent recordings of the shadows cast by anatomic structures as photons pass through the body. The principal transmission modalities include plain radiography, such as chest radiographs and abdominal radiographs, fluoroscopy, and CT. Plain radiography may be conceptualized as a snapshot: it provides a static view of anatomic structure obtained in a fraction of a second. Fluoroscopy represents a kind of "movie," or moving picture, in which continuous detection and display of the pattern of photon transmission enables the visualization of dynamic processes in real time. CT gathers transmission data from multiple perspectives and employs a mathematical algorithm

(the Fourier transform) to reconstruct an image of the slice of tissue through which the x-ray beams passed. The multidetector CT scanners being manufactured now make it possible to acquire multiple "slices" at once in a continuous fashion. In each case, the contrast in the image is a reflection of the attenuation of the x-ray beam by the tissues through which it passes. From a physical point of view, an image exhibits two crucial characteristics, contrast and detail. The level of contrast between a structure and its background must be at least several percent if it is to be detected by the human eye. Through image postprocessing, rendered possible by computed radiography and digital radiography, it is often possible to adjust and optimize the level of contrast in an image and to perform such manipulations as edge enhancement. The maximum detail detectable by the unaided human eye is 10 line pairs per millimeter. Each radiologic modality has a characteristic range of detail or spatial resolution. In decreasing order, they are plain radiography, fluoroscopy, computed tomography (CT), magnetic resonance imaging (MRI), ultrasound, and nuclear medicine. Under ideal conditions, the detail captured by plain radiography is so high that magnification enhances detail, as in the detection of microcalcifications in mammography. The term noise refers to a variety of factors that detract from the information contained in an image. Some amount of noise is inherent in every modality, but additional noise may be added by the techniques used to generate or view the image. For example, ambient light in the viewing room decreases the signal-to-noise ratio; when the overhead lights in the viewing room are turned on, many of the photons striking the observer's retina no longer carry diagnostic information. In contrast, when the overhead lights are dimmed and the only source of light is a computer monitor or the view box on which a film is mounted, the signal-to-noise ratio is maximized. Radiologists work in darkened rooms not because they fear the sun, but because they are attempting to maximize the signal-to-noise ratio.

2. Methods and Materials

Separating touching objects in an image is one of the more difficult image processing operations. The watershed transform is often applied to this problem. The watershed transform finds "catchment basins" and "watershed ridge lines" in an image by treating it as a surface where light pixels are high and dark pixels are low. Segmentation using the watershed transform works well if one can identify, or "mark," foreground objects and background locations. Marker-controlled watershed segmentation follows this basic procedure:

1. Computation a segmentation function. This is an image whose dark regions are the objects we were trying to segment.
2. Computation the foreground markers. These are connected blobs of pixels within each of the objects.
3. Computation the background markers. These are pixels that are not part of any object.
4. Modification of the segmentation function so that it only has minima at the foreground and background marker locations.

5. Compute the watershed transform of the modified segmentation function.

Steps of brain segmentation using Matlab program:

- Step 1: The Color Image and Convert it to Grayscale Reading
- Step 2: Use the Gradient Magnitude as the Segmentation Function
- Step 3: Mark the Foreground Objects
- Step 4: Compute Background Markers
- Step 5: Compute the Watershed Transform of the Segmentation Function.
- Step 6: Visualize the Result

3. The Results

This experimental study was conducted to study an accurate liver segmentation method using a parallel computing algorithm. The sample of study was included 50 patients. The main objective of this research was.

Experimental study:

Step 1: the Color Image and Convert it to Grayscale Reading as shown in figure 1.

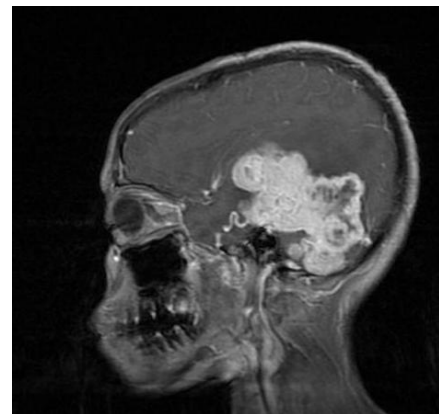


Figure 1: Shows the original image

Step 2: Use the Gradient Magnitude as the Segmentation Function. The Sobel edge masks, *imfilter*, and some simple arithmetic were used to compute the gradient magnitude. The gradient is high at the borders of the objects and low (mostly) inside the objects as shown in figure 2.

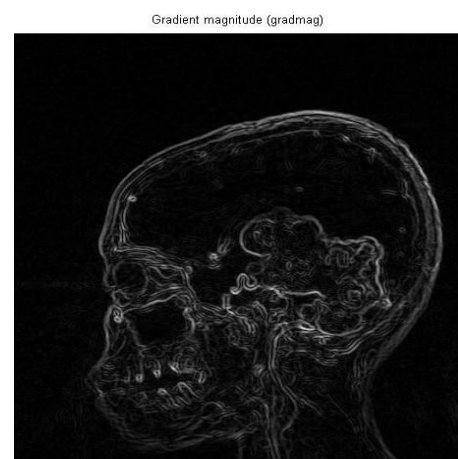


Figure 2: Gradient Magnitude as the Segmentation Function

The image was segmented by using the watershed transform directly on the gradient magnitude as shown in figure 3.

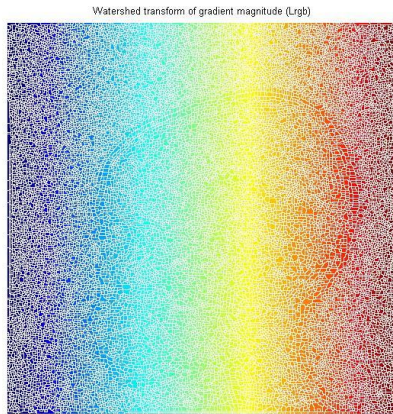


Figure 3: The watershed transform

Step 3: Mark the Foreground Objects

A variety of procedures could be applied here to find the foreground markers, which must be connected blobs of pixels inside each of the foreground objects. In this study morphological techniques were used and they called "opening-by-reconstruction" and "closing-by-reconstruction" to "clean" up the image. These operations will create flat maxima inside each object that can be located using `imregionalmax`. Opening is erosion followed by a dilation, while opening-by-reconstruction is an erosion followed by a morphological reconstruction as shown in figure 4.

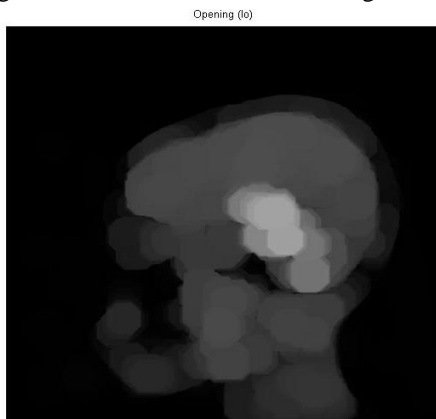


Figure 4: The Opening-by-reconstruction algorithm

Next the opening-by-reconstruction was computed using `imerode` and `imreconstruct` as shown in figure 5.



Figure 5: The opening-by-reconstruction

Following the opening with a closing can remove the dark spots and stem marks. Compare a regular morphological closing with a closing-by-reconstruction. First `imclose` code was tried as shown in figure 6.

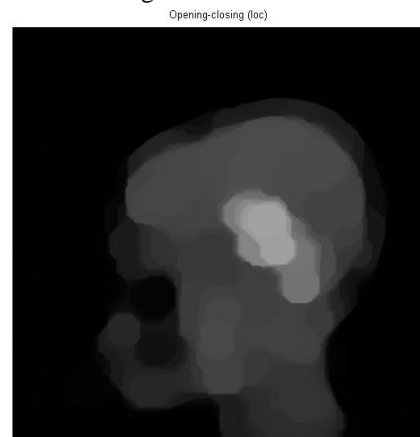


Figure 5: The 'Opening-closing algorithm

The `imdilata` code was used followed by `imreconstruct`. The image inputs and output of `imreconstruct` should complement as shown in figure 6.

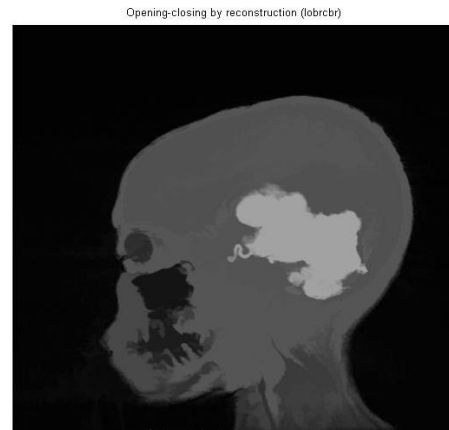


Figure 6: Opening-closing by reconstruction algorithm

When `lobrcbr` with `loc` were compared, reconstruction-based opening and closing found more effective than standard opening and closing at removing small blemishes without affecting the overall shapes of the objects. Calculate the regional maxima of `lobrcbr` to obtain good foreground markers as shown in figure 7.

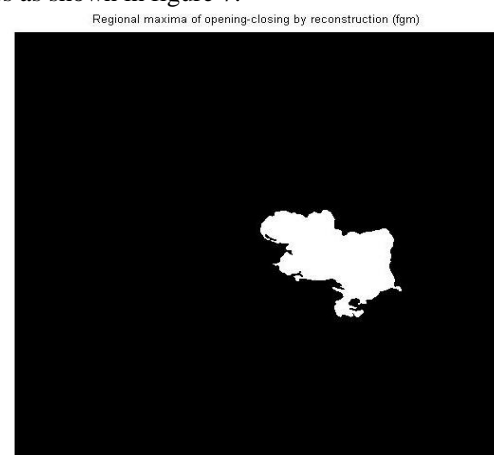


Figure 7: Regional maxima of opening-closing

To help interpret the result, superimpose the foreground marker image on the original image as shown in figure 8.



Figure 9: Regional maxima superimposed technique on original image

Some of the mostly-occluded and shadowed objects are not marked, which means that these objects will not be segmented properly in the end result. Also, the foreground markers in some objects go right up to the objects' edge. The edges of the marker blobs should clean and then shrink them a bit. This could be done by a closing followed by erosion. This procedure tended to leave some stray isolated pixels that must be removed. This could be done using `bwareaopen`, which removed all blobs that had less than a certain number of pixels as shown in figure 10.



Figure 10: Modified regional maxima superimposed on original image

Step 4: Compute Background Markers

Now the background need to be marked. In the cleaned-up image, `Iobrcbr`, the dark pixels belong to the background, a thresholding operation could start with as shown in figure 11.



Figure 11: Thresholded opening-closing by reconstruction

The background pixels are in black, but ideally the background markers shouldn't be too close to the edges of the objects which would segment. the background would "thin" by computing the "skeleton by influence zones", or SKIZ, of the foreground of bw. This can be done by computing the watershed transform of the distance transform of bw, and then looking for the watershed ridge lines ($DL == 0$) of the result.

Step 5: Compute the Watershed Transform of the Segmentation Function.

The function `imimposemin` can be used to modify an image so that it has regional minima only in certain desired locations. Here `imimposemin` used to modify the gradient magnitude image so that its only regional minima occur at foreground and background marker pixels. Finally we are ready to compute the watershed-based segmentation.

Step 6: The Result Visualization

One visualization technique is to superimpose the foreground markers, background markers, and segmented object boundaries on the original image. Dilation could use as needed to make certain aspects, such as the object boundaries, more visible. Object boundaries are located where $L == 0$ as shown in figure 12 and figure 13a & b.

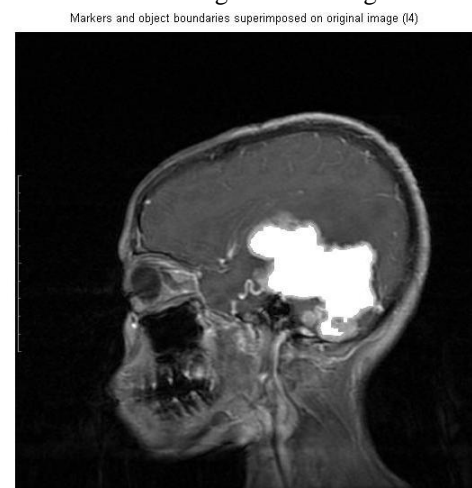


Figure 12: Markers and object boundaries superimposed on original image

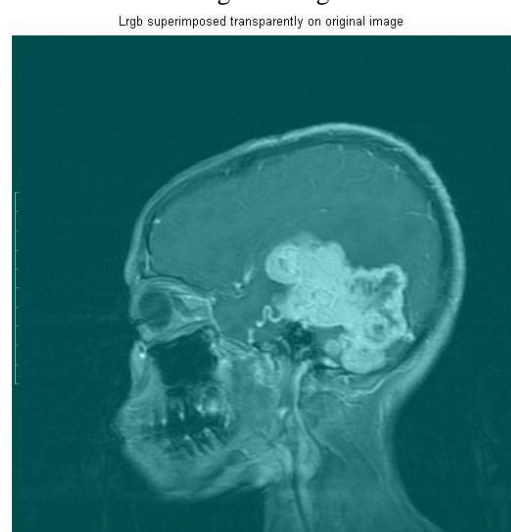


Figure 13: Segmented brain tissues colored watersheded label matrix

4. Conclusion

This experimental study was conducted to study an accurate brain tissues segmentation method using a parallel computing algorithm in MRI images. In addition to evaluate the usage of new nonlinear approach for contrast enhancement of soft tissues in MRI images in order to study automatic extraction of brain. In image processing, filters are mainly used to suppress either the high frequencies in the image, i.e. smoothing the images or the low frequencies, i.e. enhancing or detecting edges in the image. Due to various factors the images are in general poor in contrast. Researchers applied image pre-processing to remove artefacts and degradations such as blurring and noise. A variety of smoothing filters have been developed that are not linear. While they cannot, in general, be submitted to Fourier analysis, their properties and domains of application have been studied extensively. For this reason researchers applied anisotropic filtering and median filtering. In study method anisotropic and median filtering algorithms were used.

References

- [1] Abdallah YMY. Wagiallah EW. 2014. Segmentation of Thyroid Scintigraphy Using Edge Detection and Morphology Filters, International Journal of Science and Research. Volume 3, Issue 11, pp.2768-2771
- [2] Abdallah YMY. Wagiallah EW. 2014. Enhancement of Nuclear Medicine Images using Filtering Technique, International Journal of Science and Research. Volume 3, Issue 8, pp.916-921
- [3] Wagiallah EW. Ahmed Y. Abdallah YMY. 2014. Correction Preprocessing Method for Cardiac Scintigraphy Images using Local Adaptive Filters, International Journal of Science and Research. Volume 3, Issue 8, pp.1885-1889
- [4] Abdallah YMY. Abdelwahab RI. 2014. Application of Texture Analysis Algorithm for Data Extraction in Dental X-Ray Images, International Journal of Science and Research. Volume 3, Issue 8, pp.1934-1937
- [5] Adam MJ, Wilbur DS .2005. Radiohalogens for imaging and therapy. Chem Soc Rev 34:153–63
- [6] Adelson, E.H., Bergen, J.R. 1991. "The plenoptic function and the elements of early vision", In Computation Models of Visual Processing, M. Landy and J.A. Movshon, eds., MIT Press, Cambridge, 1991, pp. 3-20.
- [7] Arvo, J., 1994, The Irradiance Jacobian for Partially Occluded Polyhedral Sources, Proc. ACM SIGGRAPH, ACM Press, pp. 335-342.
- [8] Ball, J., Moore, A., 1997, Essential physics for radiographers, 3rd edition, Blackwell Scientific, Oxford.
- [9] Ball, J., Price, T., 1995, Chesney's radiographic imaging, 6th edition, Blackwell Scientific, Oxford.
- [10] Buehler, C., Bosse, M., McMillan, L., Gortler, S., Cohen, M., 2001, Unstructured Lumigraph rendering, Proc. ACM SIGGRAPH, ACM Press.
- [11] Farr, R., Allisy-Roberts, P., 1997, Physics for medical imaging, W.B. Saunders, London.
- [12] Fritsch D.S.; Chaney E.L.; McAuliffe M.J.; Raghavan S.; Boxwala A.; Earnhart J.R.D., 1995, International

Journal of Radiation Oncology, Biology, Physics, Volume 32, Number 971, , pp. 217-217.

- [13] Georgiev, T., Zheng, C., Nayar, S., Curless, B., Salesin, D., Intwala, C., 2006, Spatio-angular Resolution Trade-offs in Integral Photography, Proc. EGSR .

Author Profile



Yousif Mohamed Yousif Abdallah received the B.S., M.Sc. and PhD degrees and M.Sc. in nuclear medicine and Radiotherapy Technology from College of Medical radiological Science, Sudan University of Science and Technology in 2005, 2009 and 2013, 2014, respectively. During 2006 up to 2015, he was staying in College of Medical radiological Science, Sudan University of Science and Technology. He is now assistant professor and Consultant Radiation Therapist.

Amel A. Algaddal received the B.Sc. in College of Medical Radiological Science, Sudan University of Science and Technology. She has M.Sc. in medical diagnostic ultrasound from Sudan University of Science and Technology. She is working in Sebha Infertility Center, Sebha, Libya.

Mommen A. Alkhir is assistant professor in Sebha Infertility Center, Sebha, Libya.